Coaxial Antenna Array for 915 MHz Interstitial Hyperthermia: Design and Modelization—Power Deposition and Heating Pattern—Phased Array

Jean-Christophe Camart, Jean-Jacques Fabre, Bernard Prevost, Joseph Pribetich, and Maurice Chive

Abstract—**Coaxial antennas different in their active length have been designed, to be used in a complete 915 MHz hyperthermia system with temperature control by microwave radiometry. Heating patterns are reconstructed from the power deposition associated with the bioheat transfer equation. Temperature control is effected by means of microwave radiometry and used in order to determine bioheat parameters. Phased arrays are studied allowing heated volume expansion.**

Introduction

HEATING by means of microwaves is now a well known technique used in cancer treatment in association with radiotherapy [1]. The advantage of microwaves is that the heated volume coupled with the applicator used is well defined. In the case of deep and semi-deep tumors it appears very interesting to deposit the power directly inside the tumor. For this purpose microwave interstitial hyperthermia uses miniature antennas inserted in the same catheters implanted for brachytherapy. The first work performed was to design a complete choice of antennas different in their active length to heat tumors of different sizes and shapes. Our antennas must be simple to construct and simple to use needing no matching system (stub). Once designed by computing and measuring the reflection coefficient in the input plane, these antennas are completely characterized; this study follows these successive steps:

- theoretical determination of the radiating pattern at the heating frequency
- confirmation through electrical and thermal measurements
- theoretical determination of the pattern which contributes to the noise power
- picked up by one antenna used as a receiver associated with a 3 GHz or 9 GHz radiometer
- through field composition the study of antenna arrays is achieved
- the knowledge of the radiating pattern is used in conjunction with the bioheat transfer equation in order to determine heating patterns within the array
- using the antenna modelling when used as a radiometric receiver, the parameters in the bioheat transfer equation are determined more accurately. So heating patterns can be reconstructed at any moment of a heating session from the recorded parameters.

Results are displayed on a desktop computer as heating patterns in a cross section plane; the CPU time is not prohibitive and allows the use of software to determine a dosimetry. Phase I and II trials have been achieved; for several of them an *a priori* dosimetry has been computed, confirmation of the efficiency of the dosimetry has been given by comparison between calculated temperatures and measurements using implanted thermocouples. In a theoretical study, using our designed software, power deposition diagrams and heating patterns have been computed when one antenna is fed by a current with phase difference with regards to the others. We have then proven that it is possible to optimize the phase value and the rotation period (feeding each antenna consecutively) in order to increase the heated volume.

Materials and Methods

Antenna Geometry and Design

In order to be inserted in the same plastic catheter used for Iridium wire brachytherapy (int diameter ~ 1.1 mm) our antennas are made with UT 34 semi rigid coaxial cable 0.034 inch in external diameter (0.85 mm). The active length is achieved at the end of the cable by removing the outer conductor on a length h and completely stripping the central conductor on a length h' (Fig. 1).

This technique gives a radiating antenna of active length of about $2(h + h')$. The other end of the cable is soldered to a miniature cable connector (SMA standard) so the applicator-antenna is 25 cm long. The point $z = o$ at which the outer conductor is removed is called the junction point. The antenna is inserted in the catheter used for brachytherapy; this catheter can be filled or not with water (Fig. 1). The aim of the optimization is to develop radiating antennas that will, during use, make it possible to transfer

Manuscript received July 10, 1992; revised July 30, 1992.

J.-C. Camart, J.-J. Fabre, J. Pribetich, and M. Chive are with I.E.M.N, U.M.R. CNRS 9929, Universite-des Sciences et Technologies de Lille, Bât. P4-59655 Villeneuve d'Ascq Cedex, France.

B. Prevost is with Centre de lutte contre le Cancer Oscar Lambret-B.P. 307-59020 Lille Cedex, France.

IEEE Log Number 9203681.

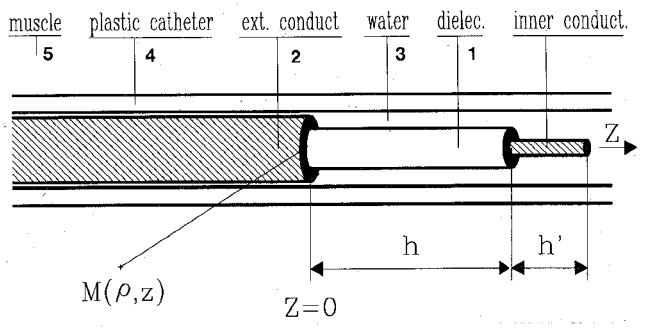

Fig. 1. Description of a radiating antenna made from a coaxial cable inserted in an implanted plastic catheter. Identification of the various regions accounted for in the theoretical calculation and referred to by numbers.

at least 90% of the microwave energy to the volume to be heated. This matching is studied by the evolution of the power reflection coefficient (S_{11} parameter) versus the frequency in the input plane of the applicator. The matching must be obtained not only at the heating frequency (915 MHz) but also in wide bandwidths around 3 and 9 GHz central frequencies of the radiometers for temperature measurement.

The theoretical approach is based on the modelling of the antenna by a dipole [2], the calculations are presented in Appendix I. Confirmation of this approach is made through measurements on a network analyzer (HP 8510A). The studied antenna is inserted in a plastic catheter and implanted in polyacrylamid gel; the insertion depth of the junction point in the medium is always greater than $h + h'$ in order to avoid any mismatching caused by the gel surface. Systematic studies have been done for h and h' values in a frequency range from 400 to 10 400 MHz.

Radiating Field of the Antenna

From a theoretical point of view, an electromagnetic field is generated in all the concentric media around the central conductor. This field is determined at any point of the volume around the antenna by two components due to the cylindrical symmetry. Following CASEY's calculations [3] we have made a numerical computation by a N points Gaussian quadrature formula of the two integrals (see Appendix I) in cylindrical coordinates giving access to $E_z(\rho, z)$ and $E_\rho(\rho, z)$ at any point $M(\rho, z)$ of the volume to be heated.

The deposited power is directly related to the squared value of the electric field module, so results are presented as SAR around the antenna applicator. Calculations have been made at the heating frequency 915 MHz and at 3 and 9 GHz central frequencies of the radiometers we use for temperature measurement. Confirmation of this theoretical approach is given by experimental determination of the radiating diagram. The first technique uses a field mapping system [4] (Fig. 2) for which the applicator antenna under test is placed in water containing six grams of salt per liter (6g/L) and fed by microwave power delivered by a generator. An electric field probe connected

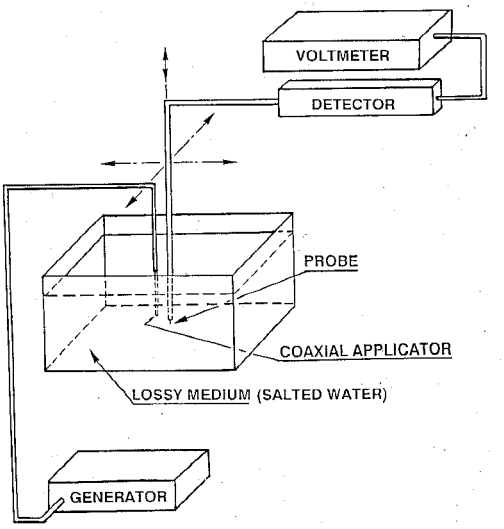

Fig. 2. Field mapping system: through a dipole antenna (parallel to the coaxial antenna, 1.5 mm long, make from UT 85 cable) the detector gives the display of a voltage directly related to the deposed power proportional to $|E|^2$.

to a square law detector measures a quantity V_{det} which is proportional to the squared field intensity E^2. The second method is achieved by measuring the temperature variation in a polyacrylamid gel which has been briefly heated (1 minute) with a high microwave power.

Temperature measurements are achieved by means of several thermocouples moved in the gel by an automatic system: the thermocouples are slid into implanted catheters only after the heating period is over and the power switched off, to avoid the problems of thermocouple-microwave interaction [5]. Brief heating and rapid measurement are necessary in order to avoid conduction phenomena in the gel. These two techniques give the SAR pattern characterized by the active length and the penetration depth (in a direction perpendicular to the antenna axis).

Using the Antenna for Temperature Measurement

Following Planck's law an elementary subvolume dv emits spontaneously a noise power dp, in a bandwidth Δf given by

$$dp = \alpha k T(x, y, z)\, \Delta f\, dv.$$

In this formula, deduced from the Nyquist law, α (Neper m^{-1}) is the power attenuation of a T.E.M. wave propagating in the medium under experiment, k is the Boltzman constant, $T(x, y, z)$ in Kelvin is the temperature of the subvolume placed in $M(x, y, z)$. When picked up by a non-ideal antenna characterized by its contribution patterns to the picked up power Ant (x, y, z), the noise power becomes

$$dp = \alpha k T(x, y, z)\ \text{Ant}\ (x, y, z)\ \Delta f\, dv.$$

By integration, the total noise power picked up by the antenna is then calculated. This power can be expressed as a temperature value T_{rad} (in Kelvin) by a numerical cal-

ibration: in the case of a medium at a constant temperature *To* (in Kelvin) the radiometric temperature must be *To*; so T_{rad} is given by

$$T_{rad} = \frac{\int \alpha_k T(x, y, z)\ \text{Ant}\ (x, y, z)\ \Delta f\, dv}{\int \alpha_k\ \text{Ant}\ (x, y, z)\ \Delta f\, dv}.$$

From the experimental point of view the noise power is measured by means of a calibrated radiometer [6], the information is a weighted temperature in volume, the temperature distribution can be determined from the previous theory. We must know the contribution pattern to the measured power Ant (x, y, z): this diagram is also the deposited power diagram at the central frequency of the used radiometer, because of the reciprocity principle and because the diagram is not modified, in a first approximation, at the other frequencies of the radiometer bandwidth [7], [8].

Antenna Array

In the case of several antennas making an array which is a common clinical implantation, the total electric field is calculated at any point $M(x, y, z)$ summing up the contribution of each antenna. The first hypothesis we made is that the current distribution of one antenna is not modified by the electromagnetic fields radiated by the others; so the distance between two antennas must be greater than 2 or 3 penetration depth. The second hypothesis is that the antennas are parallel.

In order to confirm the theoretical approach, the first calculations and experimental measurements have been done in the case of a four antenna array, the junction point $(z = o)$ of each antenna is in a cross section plane (xOy) perpendicular to the antenna direction (Fig. 6). Because the maximum deposited power is sited in the cross section plane all the reconstructions are calculated in this plane (but are also available in other planes).

Heating Pattern Reconstruction

From the knowledge of the electric field the absorbed power density is given by

$$Q = \frac{\sigma}{2} |E|^2$$

Where σ is the electrical conductivity of the biological tissue ($\sigma = 1$ S.m^{-1}). This value is reported in the following bioheat transfer equation:

$$\rho c \frac{\partial T}{\partial t} = k_t \nabla^2 T + v_s(T_a - T) + Q_m + Q.$$

In this equation ρ is the density of living tissues, c the specific heat ($\rho c = 4.18\ 10^6$ J m^{-3} °C^{-1}), k_t the thermal conductivity ($kt = 0.45$ W m^{-1} °C^{-1}) v_s the blood heat exchange coefficient, T_a the arterial temperature ($T_a = 37.3$°C), Q_m the power generated by metabolic processes

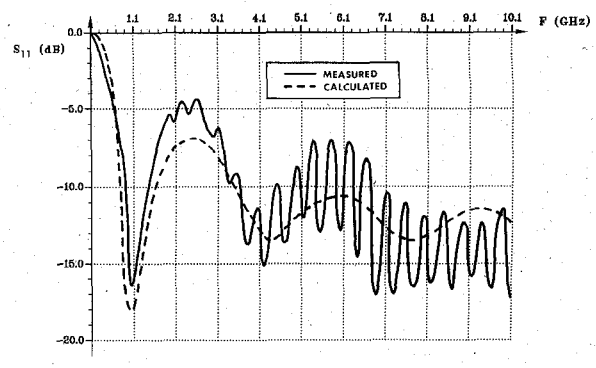

Fig. 3. Reflection coefficient calculated and measured in the input plane of the coaxial antenna implanted in polyacrylamid gel as a function of frequency for a value $h = 25$ mm and $h' = 3$ mm; the catheter is filled with water.

(Q_m is insignificant compared with Q). Except v_s, all these terms are constant and found in previous publications. The heat transfer equation is numerically solved by the Crank–Nicholson method for the time and then for each value of t, the residual elliptic equation is solved by Choleski method [9]. The corresponding software is used in a loop, for a v_s adjustment from a comparison between calculated and measured radiometric temperature. The flowchart of this software is presented in the Appendix II block diagram. Results are presented as heating patterns in cross section planes especially in the junction plane where the maximum occurs. When used in the case of polyacrylamid gel parameters value are changed as followed: ρc unchanged, $k_t = 0.38$ W m^{-1} °C^{-1}, $T_a = 20$°C, $v_s = 1500$ W m^{-3} °C^{-1} (v_s takes into account heat exchange through antennas, catheters and thermocouples).

Phased Antenna Array

In the previously designed software, feeding one antenna with a current dephased with regards to the others generates a different pattern. In a theoretical study of the radiated field of a four antenna array (presented in Fig. 6), we feed one antenna (A) with a phased current (θ°): the electric field maximum moves toward the opposite antenna. This process is used to obtain larger heated volumes within the array.

Results and Discussion

Antenna Design

The first work we carried consisted in determining the h value when $h' = o$ and the catheter is filled with air. Matching at 915 MHz imposed $h = 43$ mm, a good matching is also given around 3 and 9 GHz. The active length is then ~80 mm, because as tumors are generally smaller we had to design shorter antennas. For this purpose the catheter is filled with deionized water, the h value is chosen and the h' value is optimized in order to retain a good matching at the heating frequency. This design is made by means of a theoretical approach, only valid in a first approximation (the first antenna with a h length is linked to a second antenna with a h' length. The current

TABLE I
(h, h') VALUES GIVING GOOD MATCHING: COMPARISON BETWEEN CALCULATED AND MEASURED REFLECTION COEFFICIENT AT 915 MHz AND AROUND 3 OR 9 GHz RADIOMETRIC FREQUENCIES

		S11 (dB) 915 MHz		S11 (dB) Around 3 GHz		S11 (dB) Around 9 GHz	
h (mm)	h' (mm)	Theoret.	Measured	Theoret.	Measured	Theoret.	Measured
14	7	−21	−18	−10	−7	−12	−11
20	5	−19	−17	−11	−9	−12	−12
25	3	−18	−16	−11	−9	−12	−14
30	0, 5	−16	−14	−11	−9	−12	−11

at the linking point is equal for both antennas) and proven by measurement on a network analyzer. An example is given in Fig. 3 showing a good agreement in frequency; the differences between the S_{11} values can be explained by the ROS in the connectors and in the cable not taken into account in the theoretical calculations. The corresponding values h and h' lengths are summarized in Table I where we can note a good agreement between the computed S_{11} value and the measured one.

From the electric field computation at any point of the irradiated volume we have deduced the isopower lines around the antenna; we have plotted them as SAR; comparison between theory and measurement is accomplished by means of a field mapping system. In Fig. 4 we present the power radiated pattern around our first studied antenna. The SAR values have been normalized to their maximum (extrapoled at the surface of the catheter) and plotted as percentile contours. We can characterize a pattern by the volume limited by the 37% SAR line. This volume is defined by the penetration depth in a cross section plane at the junction point (δ # 5 mm) and the active length (L # 6 cm). These characteristics have been confirmed by a thermal experiment on polyacrylamid gel. The case of the SAR in the frequency bandwidth around 3 GHz is presented in Fig. 5. In a first approximation the volume which contributes to the noise power picked up by the antenna is limited to a cylinder of $\frac{4}{3}(h + h')$ height and of 6 mm radius. At 9 GHz the radius is now 3 mm wide so the measured temperatures give information in the vicinity of the antenna [8]. The knowledge of this SAR patterns is confirmed in the same way, and used in heating pattern reconstruction.

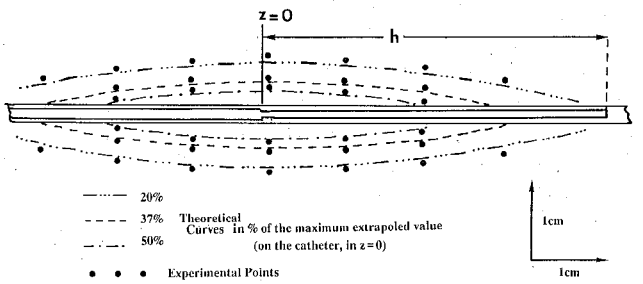

Fig. 4. Radiating diagram of the coaxial antenna for h = 43 mm, h' = 0 at 915 MHz around a catheter dipped in 6g/L salted water; theoretical lines and experimental points deduced from detected voltage obtained with the field mapping system.

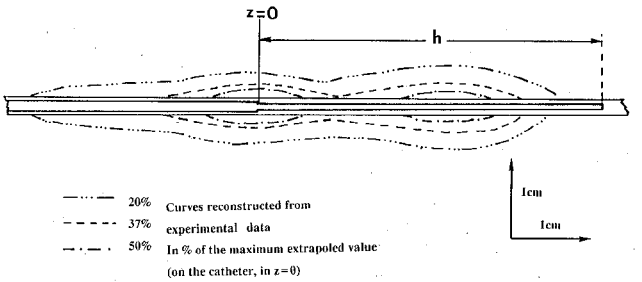

Fig. 5. Radiating diagram at 3 GHz with the same antenna in the same conditions as in Fig. 4.

Antenna Array

Brachytherapy always uses several catheters implanted inside the tumor, the distance between the catheters ranges from 10 to 18 mm. These short distances enable the composition of the electromagnetic waves [10], [11]. First calculations and experiments have been done, in a polyacrylamid gel, in the case of four antennas fed in phase. The experimental thermal SAR has been deduced from the measurement of the thermocouples (Fig. 6). We can see that the electromagnetic fields composition gives a temperature maximum (100%) in the junction plane, note also that the 37% isothermal line surrounds the four antennas. There is a good similarity between measurements and the calculated values. The results obtained were similar to those of Wong and Trembly [12]–[14]. It is however necessary to go further in the modeling so as to apply it in clinical studies taking into account blood flow. Our purpose is to reconstruct heating patterns from data recorded during a hyperthermia session. During the first experiments of the Phase I trial several thermocouples were implanted in order to have some precise temperature measurements at given points. Radiometric measurements were achieved with 3 and 9 GHz radiometer (with 0.9 GHz bandwidth). In Fig. 7 there is a good agreement between theoretical reconstruction and measured values: even the v_s value in the bioheat equation is determined from only one radiometric measurement; v_s was high in value because of the array implantation (not far from the thigh surface).

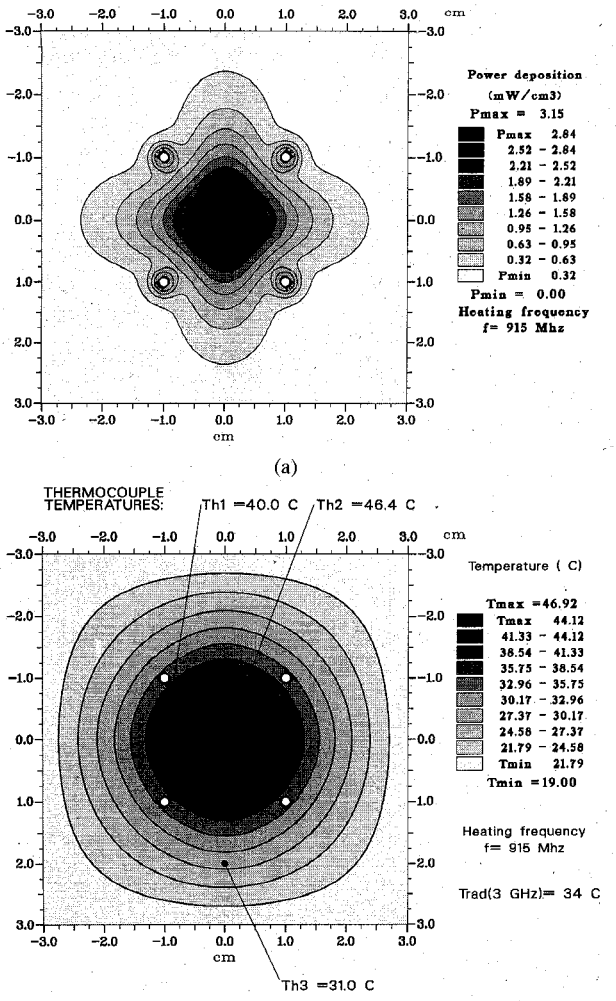

Fig. 6. Reconstructed patterns. (a) Electromagnetic field in the junction plane of a four antenna array. (b) Thermal pattern deduced from the bioheat equation.

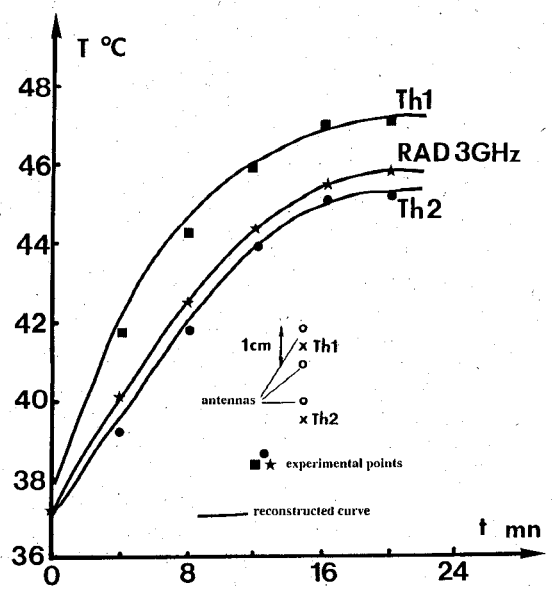

Fig. 7. Temperature evolution versus time during an hyperthermia session on a dog muscle. Comparison between measured and simulated temperatures (thermocouple and radiometric values) R = 915 MHz Pi = 12 W.

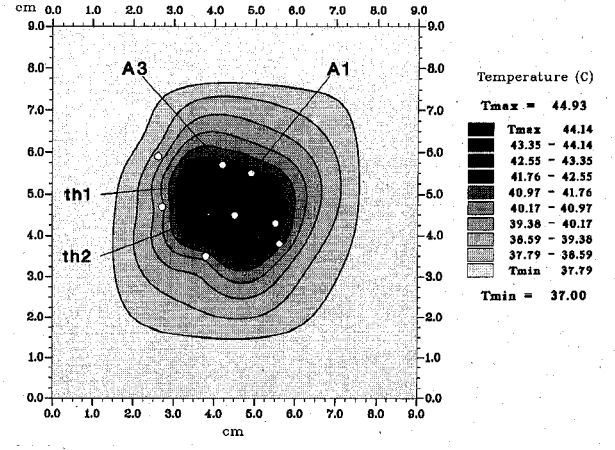

Fig. 8. Reconstructed heating patterns in the junction plane of eight antennas implanted in a base of tongue, two thermocouple measurements are reported on: $Th1$ = 41°C; $Th2$ = 42.5°C. Radiometric temperatures are measured on A1 and A3 antennas: T_{rad}(A1) = 41.5°C; T_{rad}(A3) = 42°C.

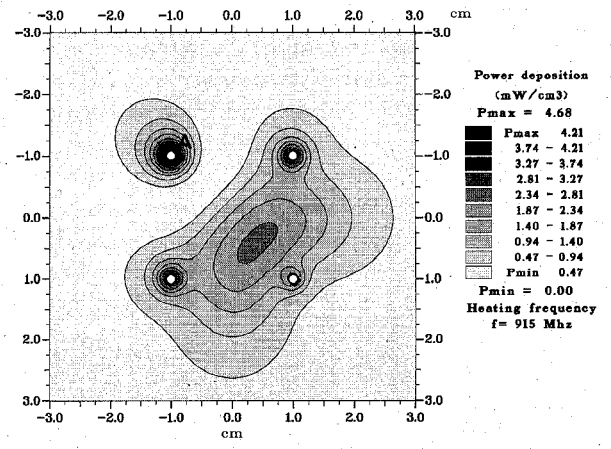

Fig. 9. Electromagnetic field reconstruction in the junction plane of a four antenna array. Antenna A is fed by a current with a phase difference value of 110° compared to the others.

In order to know how the tissues are heated it appears more interesting to display heating patterns at a given moment of the session: an example is given in Fig. 8 for a hyperthermia session on a base of tongue carcinoma: there is a difference between the temperature measured through thermocouples and computed values at the same point; this fact is due to our hypothesis: the homogeneous infinite medium is non respected in the case of the tongue. On a 33 MHz computer the display is obtained after 1 minute of calculation, in the steady state of the session, in a first approximation v_s considered as a constant, Ant (x, y, z) recorded in the computer.

Phased Array

Reconstructed patterns are the beginning of the systematic study of the phase monitored antenna array. In Fig. 9 we can see the moving of the electromagnetic field maximum when one antenna is fed with a current dephased with regards to the others. This moving gives a non symmetrical heating pattern [13]. Studying this moving versus the phase value it appears that 120° ± 10° is the most

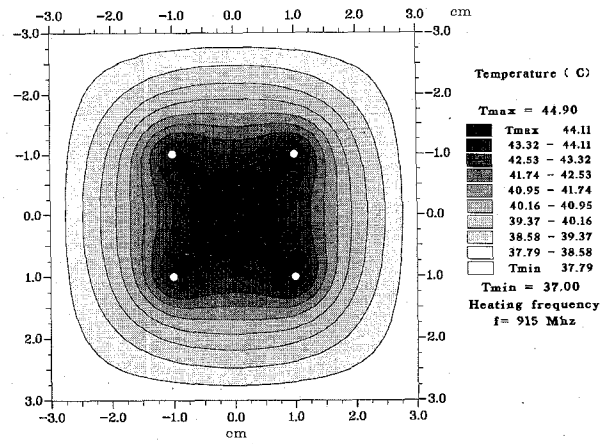

Fig. 10. Reconstructed heating patterns in the junction plane rotating 110° phased current on each antenna consecutively within a period of 4 seconds.

appropriate value for our purpose: avoiding hot spots on one antenna but keeping a sufficient temperature level in the middle of the array, we have then fed each antenna one after the other with this dephased current and optimized the rotation period τ in order to homogenize the temperature within the array. $\tau = 4$s gives access to the largest heated volume. In this case the heated volume is expanded in 300% ratio with regards to those obtained with four antennas fed in phase (Fig. 10).

Conclusion

From the theory of a symmetric dipole antenna implanted in a dissipative dielectric medium, we have designed coaxial antennas of different active lengths. Our study gives access to the SAR around one antenna and within antenna arrays. This theoretical approach is confirmed through experimental measurements and then applied in temperature reconstruction (evolution versus time or heating pattern at a moment).

From the simulation we have proven the efficiency of feeding the antennas of the array successively with a phase delayed current. This technique gives a heated volume expansion of 300%. Our antennas and reconstruction software are used in a complete hyperthermia system [15], its efficiency has been confirmed in a phase II clinical trial in tests spanning 2 years (over 50 patients) [16].

Appendix I

For an antenna of denuded part h, with ω the angular frequency, μ_0 the magnetic permeability. The reflection coefficient in the antenna input plane is expressed by

$$S_{11}\ \text{dB} = 20 \log \left[\left| \frac{Z_0 - 50}{Z_0 + 50} \right| \right]. \tag{1}$$

Where Z_0 stands for the impedance observed at the function point $z = 0$ of the antenna, and calculated from the transmission line theory:

$$Z_0 = \frac{jZ_c^*}{\tan (k_L h)}. \tag{2}$$

Z_c^* represents the complex characteristic impedance of the antenna taking into account the various surrounding conditions as noted in Fig. 1, k_L is the wave number characterizing the energy propagation in the antenna, when the following hypotheses are respected we can calculate Z_c^* and k_{2e}:

$$\left[\frac{k_5}{k_4}\right]^2 \gg 1;\ (b.k_2)^2 \ll 1;\ (c.k_3)^2 \ll 1;\ (d.k_4)^2 \ll 1;\ a \ll h.$$

From the wave numbers can then be calculated coefficients analogous to refraction indexes:

$$n_{23}^2 = \left[\frac{k_2}{k_3}\right]^2; \quad n_{24}^2 = \left[\frac{k_2}{k_4}\right]^2; \quad n_{25}^2 = \left[\frac{k_2}{k_5^*}\right]^2.$$

A wave number equivalent to two successive media k_{2e} is then introduced by

$$k_{2e} = k_2 \left[\frac{\text{Ln}\ (d/a)}{\text{Ln}\ (b/a) + n_{23}^2\ \text{Ln}\ (c/b) + n_{24}^2\ \text{Ln}\ (d/c)} \right]^{1/2}$$

The condition $[k_5/k_{2e}]^2 >> 1$ is a-posteriori verified allowing to employ this theory, which enables to express the wave number k_L characterizing the energy propagation in the antenna:

$$k_L = k_{2e} \left[\frac{\text{Ln}\ (d/a) + F}{\text{Ln}\ (b/a) + n_{25}^2.F} \right]^{1/2}.$$

The complex characteristic impedance is then expressed as

$$Z_c^* = \left[\frac{\omega \mu_O k_L}{2\pi k_{2e}^2} \right] \cdot [\text{Ln}\ (d/a) + n_{2e5}^2 F] \tag{3}$$

where

$$n_{2e5}^2 = \left[\frac{k_{2e}}{k_5^*}\right]^2 \text{ and}$$

$$F = \frac{H_O^{(1)}(k_5.d)}{k_5.d.H_1^{(1)}(k_5.d)}\ H\text{: Hankel function}$$

The electric field can then be expressed by two components due to the cylindrical symmetry, at the observation point defined by ρ and z, coming from a source point

defined by ρ', z', ϕ':

$$E_{5z}(\rho, z) = \frac{1}{4\Pi} \frac{I(o)}{2\Pi \sin k_L h} \cdot \left[-2j\omega\mu_O \int_{-h}^{h} \int_{0}^{\pi} \cdot \sin k_L(h - |z'|) \frac{e^{-jk_5R}}{R} d\Phi' \, dz' \right.$$

$$-2j\omega\mu_O \, d \, \mathrm{Ln}\left(\frac{d}{a}\right)\left(1 - \frac{k_L^2}{k_{2e}^2}\right) \int_{-h}^{h} \int_{0}^{\pi} \cdot \sin k_L(h - |z'|) \frac{e^{-jk_5R}}{R^2}\left(\frac{1}{R} + jk_5\right) (d - \rho \cos \Phi') \, d\phi' \, dz'$$

$$+ \frac{2jk_L}{\epsilon_5^* \omega} \int_{-h}^{O} \int_{O}^{\pi} (z - z') \cdot \cos k_L(h + z') \frac{e^{-jk_5R}}{R^2}\left(\frac{1}{R} + jk_5\right) d\phi' \, dz'$$

$$- \frac{2jk_L}{\epsilon_5^* \omega} \int_{0}^{h} \int_{O}^{\pi} (z - z') \cdot \cos k_L(h - z') \frac{e^{-jk_5R}}{R^2}\left(\frac{1}{R} + jk_5\right) d\phi' \, dz' \left.\right]$$

and

$$E_{5\rho}(\rho, z) = \frac{1}{4\Pi} \frac{I(o)}{\Pi \sin k_L h} \cdot \left[-j\omega\mu_O \, d \, \mathrm{Ln}\left(\frac{d}{a}\right)\left(1 - \frac{k_L^2}{k_{2e}^2}\right) \int_{-h}^{h} \int_{O}^{\pi} \cdot \sin k_L(h - |z'|) \frac{e^{-jk_5R}}{R^2}\left(\frac{1}{R} + jk_5\right) (z - z') \cos \Phi' \, d\Phi' \, dz' \right.$$

$$- \frac{jk_L}{\epsilon_5^* \omega} \int_{-h}^{O} \int_{O}^{\pi} \cos k_L(h + z') \cdot \frac{e^{-jk_5R}}{R^2}\left(\frac{1}{R} + jk_5\right) (d \cos \phi' - \rho) \, d\phi' \, dz'$$

$$+ \frac{jk_L}{\epsilon_5^* \omega} \int_{O}^{h} \int_{O}^{\pi} \cos k_L(h - z') \cdot \frac{e^{-jk_5R}}{R^2}\left(\frac{1}{R} + jk_5\right) (d \cos \phi' - \rho) \, d\phi' \, dz' \left.\right]$$

with

$$R = \left[(z - z')^2 + (\rho - \rho')^2 + 4\rho\rho' \sin \frac{z\phi'}{2} \right]^{1/2} \Bigg|_{\rho' = d}$$

and $I(o)$ the feeding current normalized to $1/Z_0$.

Appendix II
Flowchart of the Thermal Dosimetry Software

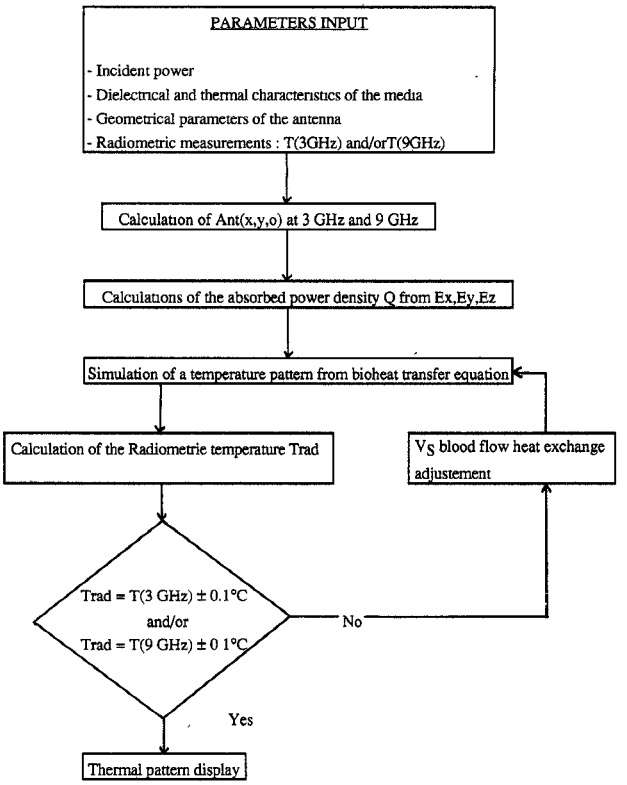

References

[1] J. M. Cosset, "Interstitial hyperthermia," in *Interstitial and Endocavitary and Perfusional Hyperthermia: Methods and Clinical Trials*, M. Gautherie Ed.: Berlin: Springer Verlag, 1990, pp. 1-37.

[2] R. W. P. King, B. S. Trembly, and J. W. Strohbehn, "The electromagnetic field of an insulated antenna in a conducting or dielectric medium," *IEEE Trans. Microwave Theory Tech.*, vol. MTT-31, pp. 574-583, 1983.

[3] J. P. Casey and R. Bansai, "The near field of an insulated dipole in a dissipative dielectric medium," *IEEE Trans. Microwave Theory Tech.*, vol. MTT-34, pp. 459-463, 1986.

[4] G. Gadja, M. A. Stuchly, *et al.*, "Mapping of the near field pattern in simulated biological tissues," *Electron. Lett.*, vol. 15, no. 4, pp. 120-121, 1979.

[5] B. J. James, J. W. Strohbehn, *et al.*, "The effect of insertion depth on the theoretical SAR patterns of 915 MHz dipole antenna arrays for hyperthermia," *Int. J. Hyperthermia*, vol. 5, no. 6, pp. 733-747, 1989.

[6] M. Plancot, B. Prevost, *et al.*, "A new method for thermal dosimetry in microwave hyperthermia using microwave radiometry for temperature control," *Int. J. Hyperthermia*, vol. 3, no. 1, pp. 9-19, 1987.

[7] M. Chive *et al.*, "Microwave hyperthermia controlled by microwave radiometry. Technical aspects and first clinical results," *J. Microwave Power*, pp. 233-241, 1984.

[8] M. Chive, "Use of microwave radiometry for hyperthermia monitoring and as basis for thermal dosimetry," in *Methods of Hyperthermia Control*, series on clinical thermology, subseries thermotherapy, vol. 3, pp. 113-128, M. Gautherie, Ed. Berlin: Springer Verlag.

[9] L. Dubois, J. Pribetich, J. J. Fabre, M. Chive, and Y. Moschetto, "Noninvasive microwave multifrequency radiometry used in microwave hyperthermia for bidimensional reconstruction of temperature patterns," *Int. J. of Hyperthermia*, to be published.

[10] Y. Zhang *et al.*, "The calculated and measured temperature distribution of a phased interstitial antenna array," *IEEE Trans. Microwave Theory Tech.*, vol. 38, no. 1, pp. 69-77, 1990.

[11] ——, "Microwave hyperthermia induced by a phased interstitial antenna array," *IEEE Trans. Microwave Theory Tech.*, vol. 38, no. 2, pp. 217–221, 1990.
[12] T. Z. Wong *et al.*, "SAR patterns from an interstitial microwave antenna-array hyperthermia system," *IEEE Trans. Microwave Theory Tech.*, vol. 34, no. 5, pp. 560–567, 1986.
[13] B. S. Trembly *et al.*, "Control of the SAR pattern within an interstitial array through variation of antenna driving phase," *IEEE Trans. Microwave Theory Tech.*, vol. 34, no. 5, pp. 568–578, 1986.
[14] ——, "Comparison of power deposition by in phase 433 MHz and phase modulated 915 MHz interstitial antenna-array hyperthermia systems," *IEEE Trans. Microwave Theory Tech.*, vol. 36, no. 5, pp. 908–916, 1988.
[15] J. J. Fabre *et al.*, "Microwave interstitial hyperthermia system monitored by microwave radiometry (HIMCAR) and dosimetry by heating pattern remote sensing," *Proc. Europ. Microwave Conf.*, Stuttgart, vol. 2, 1991, pp. 1409–1414.
[16] B. Prevost, S. De Cordoue, J. C. Camart, J. J. Fabre, M. Chive, and J. P. Sozanski, "915 MHz Microwave Interstitial Hyperthermia; part III; Phase II clinical results," *Int. J. Hyperthermia*, to be published.

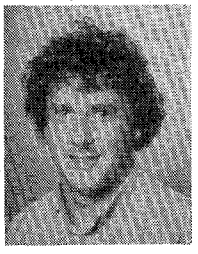

Jean-Christophe Camart was born in Lille, France in 1963. He received the M.S. degree in 1989 and the Ph.D. degree.

He works on 915 MHz applicators for interstitial hyperthermia in the Institut d'Electronique et de Microélectronique du Nord (I.E.M.N.) U.M.R. C.N.R.S. 9929. He is also a teacher at the University of Science and Technology of Lille.

Jean-Jacques Fabre was born in Lille, France on April 8, 1952. He received the M.S. degree in 1979 and the Ph.D. in 1982.

He joined the Hyperthermia Group of Lille in 1985 and has devoted full time to the design and development of microwave applicators and systems for interstitial hyperthermia in the Institut d'Electronique et de Microélectronique du Nord (I.E.M.N.) U.M.R. C.N.R.S. 9929. He is currently a lecturer at the University of Science and Technology of Lille.

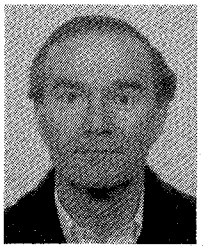

Bernard Prevost was born in Lille, France on October 30, 1947. He received medical doctorate degree from the Medicine University of Lille in 1973, then graduated in radiology and radiotherapy.

In 1976, he joined the Oscar Lambret Oncology Center of Lille (C.O.L.) as a radiotherapist. Since 1981, he has been working on medical applications of hyperthermia. He is now chief of the department (radiotherapy) at the C.O.L.

Joseph Pribetich was born in France in 1944. He received the Docteur-es-Sciences degree from the University of Lille (France) in 1979.

He is working at the Institut d'Electronique et de Microélectronique du Nord (I.E.M.N.) U.M.R. C.N.R.S. 9929 (Department Hyperfrequency and Semiconductor) on the modelling of applicators and antennas to be used in hyperthermia systems. In addition, he is a Professor of Electronics at the University of Lille.

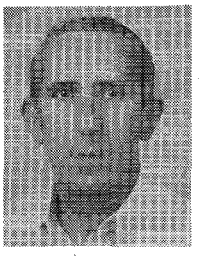

Maurice Chive was born in Lille, France on February 18, 1940. He received the Doctorate 3ème cycle in 1967, and the Doctorat-es-Sciences Physiques in 1978 from the University of Lille.

In 1968, he joined the Centre Hyperfréquences et Semiconducteurs Université de Lille, where he was concerned with research on Semiconductor devices up to 1978. Since he has been working on biomedical applications of microwaves. He is now Professor at this University and research manager of the Hyperthermia Group of Lille.